

Does Nitrogen Doping Enhance the Electrocatalysis of the Oxygen Reduction Reaction by Multiwalled Carbon Nanotubes?

Yuanyuan Lu, Xiuting Li, Archana Kaliyaraj Selva Kumar, and Richard G. Compton*



Cite This: *ACS Catal.* 2022, 12, 8740–8745



Read Online

ACCESS |



Metrics & More

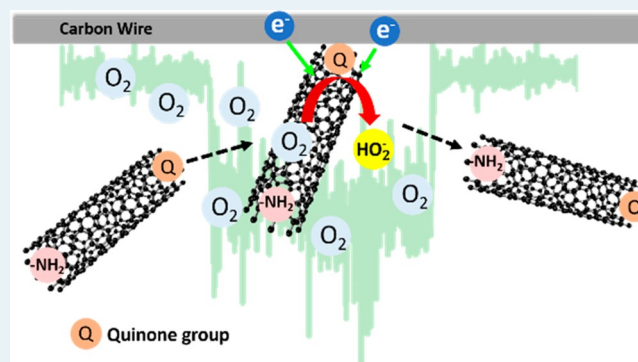


Article Recommendations



Supporting Information

ABSTRACT: Single-entity electrochemistry measurements were used to compare the electrocatalysis of the oxygen reduction reaction (ORR) by means of multiwalled carbon nanotubes (MWCNTs) or amino-functionalized multiwalled carbon nanotubes (MWCNTs-NH₂). All of the evidence showed that an electroactive surface oxygen functionality played the most important role in the catalysis process, not the nitrogen content.



KEYWORDS: oxygen reduction reaction, voltammetry, single-entity electrochemistry, MWCNTs, amino-functionalized nanotubes

The oxygen reduction reaction (ORR) is essential to the cathode of fuel cells¹ and metal–air batteries.² The ORR proceeds either through a highly efficient four-electron process to form H₂O/OH[−] or a less efficient two-step, two-electron pathway to form H₂O₂/HO₂[−] as an intermediate under acidic or alkaline conditions, respectively.³ Platinum (Pt)-based catalysts have been utilized to improve the reaction kinetics of the ORR.^{4,5} However, on consideration of the great expense, short durability,⁶ and susceptibility to deactivation⁷ of Pt, the study of low-cost carbon-based materials as ORR electrocatalysts to replace Pt in fuel cells has grown.⁸

Among these materials, carbon nanotubes (CNTs) are interesting due to their high specific surface area, chemical stability,^{9,10} and often abundant active sites,^{11,12} including edge-plane like defects and oxygen functionalities such as quinones.^{13,14} Dai et al.¹⁵ reported that nitrogen (N)-doped carbon nanotube arrays demonstrated electrocatalytic activity superior to that of Pt for the ORR in alkaline media with suggestions that the ORR electrochemical activity comes from doped impurities such as N,¹⁶ sulfur (S),¹⁷ and phosphate (P)¹⁸ and not from the carbon material. This issue has been partially resolved by the defect mechanism of carbons proposed by Zhao et al.¹⁹ that the removal of N atoms from graphene creates catalytically active defects contributing to higher ORR activity. On the other hand, similar catalytic voltammetric responses for the ORR at nondoped and N-doped carbon nanofiber (CNF) electrodes under alkaline conditions (pH >10) were observed. This suggested that the N-doped CNFs hindered the superoxide radical anion (O₂^{•−}) adsorption process, limiting the rate of hydrogen peroxide

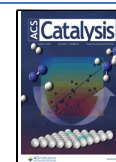
(HO₂[−]) generation.²⁰ Composites of CNTs, either undoped or doped, were used in previous studies. The complexity of unscrambling mechanistic details from such porous layers is well documented.^{21,22} Therefore, to better clarify the benefits, if any, of N doping of CNTs for promoting carbon-based materials for the ORR, multiwalled carbon nanotubes (MWCNTs) and amino-functionalized multiwalled carbon nanotubes (MWCNTs-NH₂) were studied as catalysts for the ORR at the single-entity level^{23,24} in this paper.

In previous studies, the electrocatalytic behavior of MWCNTs for the ORR in aqueous base using single-entity electrochemical techniques has been validated.^{25,26} These experiments employed a microelectrode in a suspension of CNTs, which by their Brownian motion affect the electrode randomly, allowing a voltammetric interrogation of a single tube in the medium of interest during the period, often milliseconds, in which the tube is in electrical contact with the electrode. In the following, we used nanoimpact experiments to compare the electrocatalytic behavior of MWCNTs and MWCNTs-NH₂ toward the ORR in the search for clear evidence about the role of N substitution in promoting, or not, the ORR. The experimental details are provided in Section 1 in

Received: May 19, 2022

Revised: June 22, 2022

Published: July 7, 2022



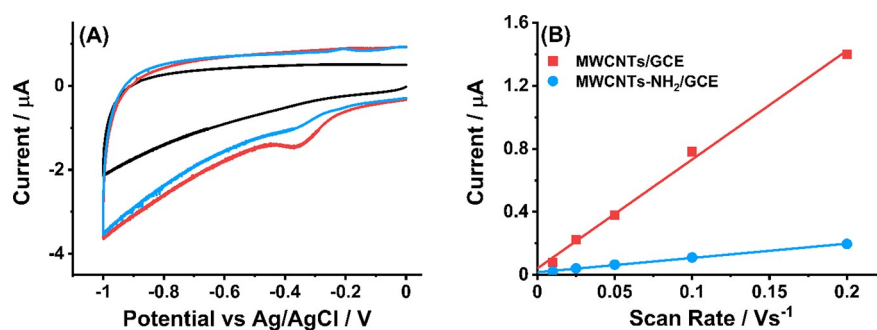


Figure 1. (A) Cyclic voltammograms measured at a bare GCE (black line) and polished GCEs modified with 0.1 μg of MWCNTs (red line) or 0.1 μg of MWCNTs-NH₂ (blue line) in the potential window from 0 V to -1.0 V at a scan rate of 50 mV s^{-1} in nitrogen-saturated 0.1 M KOH solution. (B) Comparison of the reductive peak currents observed at MWCNTs/GCE and MWCNTs-NH₂/GCE as a function of scan rate at 10, 25, 50, 100, and 200 mV s^{-1} . The cyclic voltammograms of MWCNTs/GCE and MWCNTs-NH₂/GCE at various scan rates are shown in Figure S3, respectively, and the baseline subtraction process is shown in Figure S5.

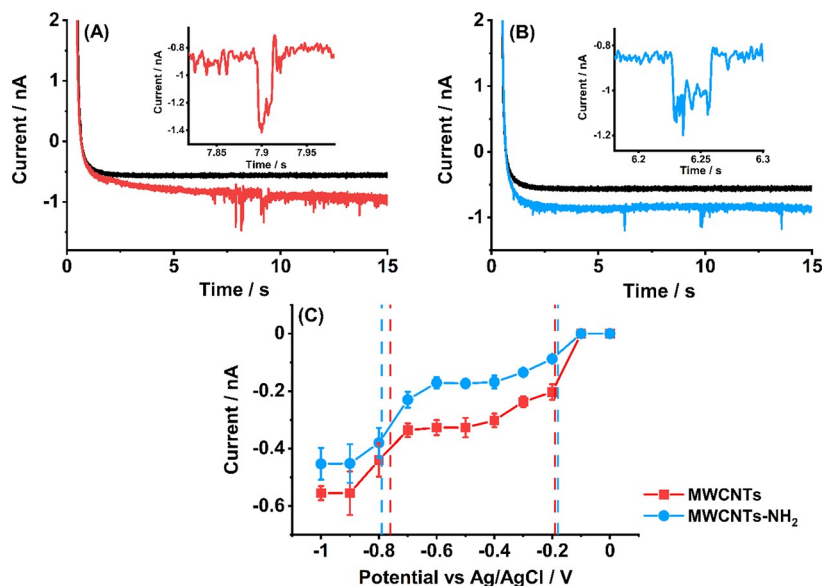


Figure 2. Representative chronoamperometric curves presenting reductive step signals at -0.4 V vs Ag/AgCl in nitrogen-degassed 0.1 M KOH in the presence of 0.001 g L^{-1} of MWCNTs (A, red line) and 0.001 g L^{-1} of MWCNTs-NH₂ (B, blue line) and in the absence of both CNTs (black line). The insets show enlargements of an individual step. (C) Plots of the corresponding average step currents produced by the collision of MWCNTs or MWCNTs-NH₂ on the carbon-microwire electrode against the applied potential from 0 to -1.0 V. The error bars represent the average of at least 40 separate impacts for each potential. Vertical lines represent the half-wave potential ($E_{1/2}$) at each step in the presence of MWCNTs (red dotted line) or MWCNTs-NH₂ (blue dotted line).

the Supporting Information. Note that the two types of CNTs have similar external surface areas per tube ($\sim 2 \times 10^{-12} \text{ m}^2$), facilitating the comparisons discussed below. The MWCNTs are formed of nine concentric tubes,²⁷ and the MWCNTs-NH₂ are comprised of six concentric tubes.²⁸

The electrochemical reduction of MWCNTs and MWCNTs-NH₂ in a degassed 0.1 M KOH aqueous solution (pH 13.3) was explored using cyclic voltammetry (CV) at a freshly polished glassy-carbon electrode (GCE) modified with 0.1 μg of MWCNTs or MWCNTs-NH₂. The coverages correspond to a ca. monolayer coverage, assuming the CNTs to be uniformly spread and arranged in a close-packed manner (see Section 2 in the Supporting Information); in reality the CNTs will aggregate, distribute heterogeneously,²⁹ and locally form thicker randomly oriented layers (Figure S2). The voltammetry is illustrated in Figure 1A. A single reductive peak appeared at -0.38 ± 0.03 or -0.37 ± 0.01 V vs Ag/AgCl ($[\text{Cl}^-] = 3.5 \text{ M}$; note that $E_{\text{RHE}} = E_{\text{X/Y}} + 0.059 \text{ pH} + E^\circ_{\text{Ag/AgCl}}$, where $E^\circ_{\text{Ag/AgCl}} = 0.1976 \text{ V}$ at 298 K and $E_{\text{X/Y}}$ is the potential

of the working electrode relative to the X/Y couple) for the MWCNTs-modified GCE (red line) or MWCNTs-NH₂-modified GCE (blue line), respectively, which is not observed at a bare GCE (black line). The reduction is assigned to surface quinones (and/or possibly other oxygen functionalities) present in the CNTs, as has been reported.³⁰ Meanwhile, the reductive peak currents for both types of CNTs showed a linear scan rate dependence (Figure 1B) consistent with the voltammetry of a surface-immobilized entity. The peak from the MWCNTs-modified GCE displays obviously larger cathodic currents in comparison to those from the MWCNTs-NH₂-modified GCE, suggesting that there are more quinones on the MWCNTs surface, since comparable numbers of CNTs were drop-casted in each case (7.7×10^6 MWCNTs and 1.8×10^7 MWCNTs-NH₂, see Section 2 in the Supporting Information). The reductive voltammetry at both types of modified GCEs is chemically irreversible (Figure S4), especially for MWCNTs-NH₂, where the quinone signal was completely absent in subsequent scans.

The electroreduction kinetics of MWCNTs and MWCNTs-NH₂ were further studied using single-entity electrochemistry with a carbon-wire microelectrode. In the presence of 0.001 g L⁻¹ of MWCNTs or MWCNTs-NH₂ in a nitrogen-saturated 0.1 M KOH solution, at least 10 chronoamperometric scans were run to record the impact steps for each applied potential within the range from 0 to -1.0 V. In Figure 2A, the appearance of the reductive step features reflected the random arrival and loss of MWCNT particles at the electrode surface with an average residence time of 0.024 ± 0.005 s. Analogous nanoimpact experiments with MWCNTs-NH₂ also demonstrated clear reductive steps at the same potential and a similar duration time (0.020 ± 0.005 s) (Figure 2B). In the absence of CNTs, the chronoamperometric current showed no impact signals, only a monotonic decay first that leveled off gradually as an indication of the capacitive charging of the electrode (black line in Figure 2A,B). The average impact current at different potentials for both MWCNTs and MWCNTs-NH₂ were calculated from at least 40 samples per potential and plotted against the applied potential (Figure 2C). For potentials more positive than -0.1 V, no reductive impacts were seen. Two current plateaus on both types of CNTs were observed: first in the potential range from -0.4 to -0.6 V and second at potentials more negative than -0.9 V. For MWCNTs, an average reductive current height of ca. 0.32 ± 0.03 nA at the first plateau and ca. 0.55 ± 0.03 nA at the second plateau were estimated; for MWCNTs-NH₂, two relatively smaller values of ca. 0.17 ± 0.02 and ca. 0.45 ± 0.06 nA respectively reflected the current response at the two plateaus. An enhanced number of reductive quinone groups of $\sim 3.3 \times 10^{14}$ molecules cm⁻² of the MWCNTs external surface was calculated from its average impact charge (2.0 ± 0.3 pC) in the first wave relative to the value ($\sim 2.4 \times 10^{14}$ molecules cm⁻²) for single MWCNTs-NH₂ (see Section 4 in the Supporting Information), assuming a two-electron process. Note that the high approximate coverages inferred indicate a contribution to the signal from some CNT aggregates. Also, it is interesting to observe that only the first single entity "wave" appeared as the single reductive peak in the CV of the modified GCEs; the absence of the second reductive peak in the CV likely resulted from depletion of active surface-bound species as a result of the chemical irreversibility of the first reduction (see above). As inferred from both ensemble and single-entity electrochemistry above and the literature,³¹ the two-step features in the nanoimpact experiments are suggested to be the formation of semiquinones (Q⁻) and quinone dianions (Q²⁻). Overall, the single-entity data in the absence of oxygen suggest more surface oxygen functionalities on MWCNTs in comparison to amino functionalized analogues.

Next, the investigation of the ORR at MWCNTs and MWCNTs-NH₂ was conducted by drop-casting the two types of materials with an amount of 0.1 μ g onto a freshly polished GCE. As shown in Figure 3, in oxygen-saturated 0.1 M KOH, similar voltammetric features were observed for three electrodes, a bare GCE and MWCNTs- or MWCNTs-NH₂-modified GCEs in the potential window from 0 to -1.4 V vs Ag/AgCl: two reductive peaks at -0.58 ± 0.01 V (Peak₁) and -0.82 ± 0.05 V (Peak₂). The voltammetric behavior of both peaks on a bare GCE reflected an overall two-electron reduction from oxygen to peroxide due to the formation of surface-adsorbed hydroperoxide species at high pH, as described in previous studies.^{32,33} In comparison with the bare GCE, the CV response of the two modified GCEs demonstrated higher

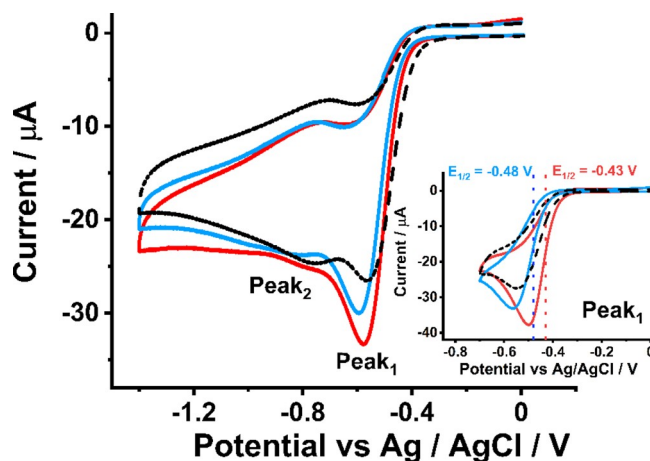


Figure 3. Cyclic voltammograms of the bare GCE (black dotted line), MWCNTs-modified GCE (red dashed line), and MWCNTs-NH₂-modified GCE (blue dashed line) in oxygen-saturated 0.1 M KOH. Scan rate: 50 mV s⁻¹. Inset: CV scanned from 0 to -0.7 V, where the vertical dotted line represents the half-wave ($E_{1/2}$) for the ORR in the presence of MWCNTs (red) or MWCNTs-NH₂ (blue).

currents for Peak₁, with the MWCNTs-modified GCE showing the largest current for both peaks. The peak currents of Peak₁ and Peak₂ obtained from MWCNTs/GCE and MWCNTs-NH₂/GCE were respectively studied as a function of scan rate, where both magnitudes were found to scale linearly with the scan rate on a logarithmic scale (Figure S6) as an indication of diffusional responses. The enhancement of the peaks may be caused by the change in diffusion from semi-infinite at the bare electrode to a thin layer with the porous layer formed by drop-casting CNTs on the electrode surface. In a focus on Peak₁ by narrowing the sweeping potential range to -0.7 V (inlay of Figure 3), the signal at the MWCNTs/GCE showed a slightly lower peak potential ($E_{c1} = -0.50 \pm 0.01$ V) in comparison to that at the MWCNTs-NH₂/GCE ($E_{c2} = -0.56 \pm 0.04$ V), suggesting the enhanced catalytic ability of MWCNTs.

Having compared the catalytic ability of the MWCNTs and MWCNTs-NH₂ toward ORR in ensemble electrochemistry, we conducted single-entity experiments on both types of individual CNT particles. A clean carbon fiber microwire electrode (diameter ca. 7 μ m and length ca. 1 mm) was inserted into an oxygen-saturated 0.1 M KOH solution containing 0.001 g L⁻¹ of MWCNTs or MWCNTs-NH₂ before chronoamperometric scans at -0.4 V vs Ag/AgCl; clear reductive steps were seen and associated with the ORR at a single MWCNT or MWCNT-NH₂ (Figure 4A) randomly impacting on the electrode surface with different average residence times of 0.083 ± 0.016 and 0.043 ± 0.015 s, respectively. The average impact current (3.6 ± 0.4 nA from 43 impacts) for the MWCNT particle was higher than the value (1.8 ± 0.2 nA from 40 impacts) for the MWCNT-NH₂ particle. In the absence of any CNT particles, only capacitive charging of the microwire electrode was observed (Figure S7).

Impacts were explored at various potentials from 0.1 to -1.0 V. Typical chronoamperometric curves recorded at -1.0 V for MWCNTs and MWCNTs-NH₂ are shown in Figure 4B. Figure 5 shows the average Faradaic current for each CNT versus the applied potential; two plateaus were seen, reflecting the current-potential characteristics for the ORR. The average currents at the two plateaus were 3.7 and 8.6 nA for a MWCNT, while lower plateaus were seen at a single MWCNT-

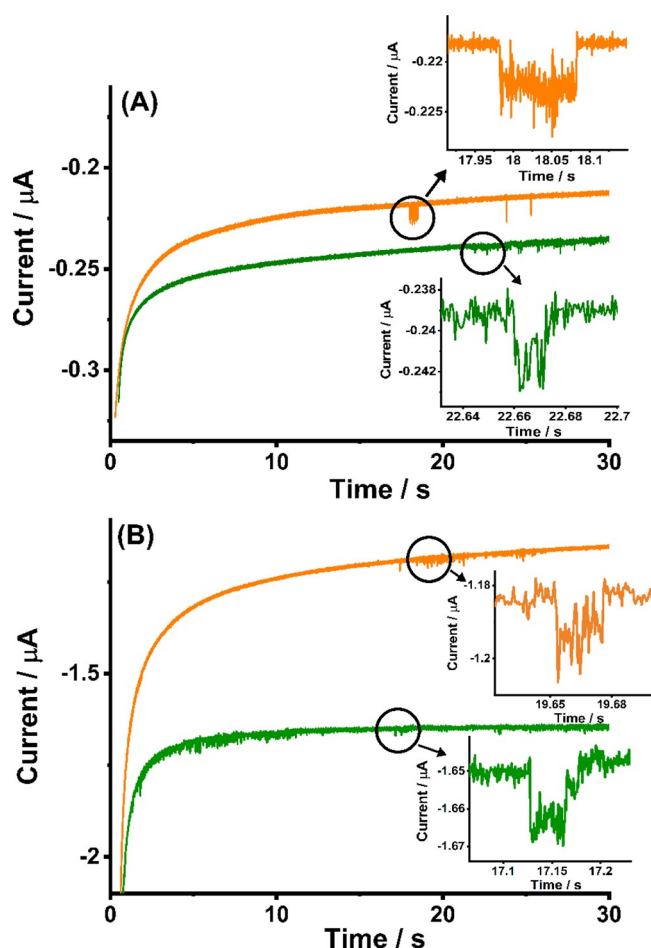
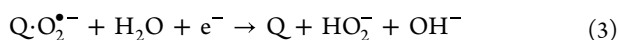


Figure 4. Representative chronoamperometric profiles showing impact signals in oxygen-saturated 0.1 M KOH at -0.4 V (A) or -1.0 V vs Ag/AgCl (B) in the presence of 0.001 g of MWCNTs (orange line) or MWCNTs-NH₂ (blue line). Insets: the corresponding enlarged impact steps.

NH₂; namely, 2.7 and 7.2 nA. Using a cylindrical electrode geometry to approximate the diffusion-limiting current on a single CNT and assuming an overall two-electron process, this was estimated to be ~ 8 nA for MWCNTs and ~ 18 nA for MWCNTs-NH₂ (Section 7 in the Supporting Information) with the chemistry assumed to be as follows.³⁵

First reduction:



Second reduction:



The values of the plateau currents suggest that the reduction via the dianion route brings about the ORR at a rate near the diffusion-controlled reduction of oxygen. In contrast, the amino-derivatized CNTs are less effective; as was discussed above, the latter contain fewer quinone functionalities. Meanwhile, in the single-entity "voltammograms", the half-wave potentials for the first wave were -0.28 ± 0.02 and -0.36

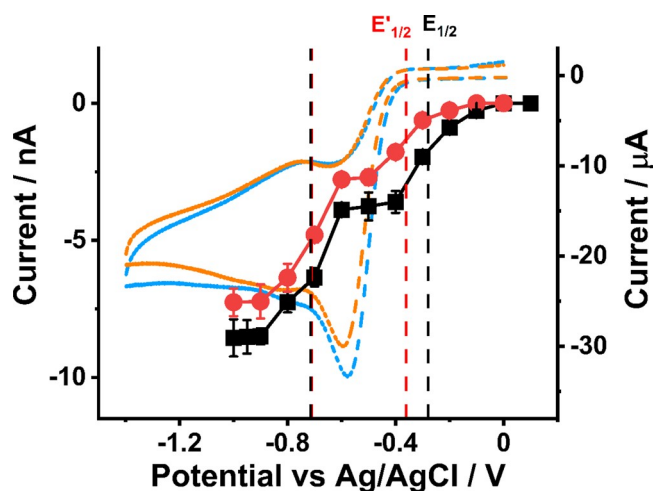


Figure 5. Potential dependence of the average impact currents for ORR catalyzed by a single MWCNT (black dots) or MWCNT-NH₂ (red dots) using a carbon-wire microelectrode. Shown for comparison are CVs recorded at a MWCNTs-modified GCE (blue line) and a MWCNTs-NH₂-modified GCE (orange line) for the ORR at a scan rate of 50 mVs^{-1} . Vertical dashed lines represent the half-wave potential ($E_{1/2}$) at each step in the presence of MWCNTs (black dotted line) or MWCNTs-NH₂ (red dotted line).

± 0.005 V for MWCNTs and MWCNTs-NH₂, respectively, which are cathodic of the consistent value of -0.19 ± 0.01 V seen in the absence of oxygen. The cathodic shift in the presence of oxygen suggests that the oxygen complexes with the quinone before the electrochemically reversible electron transfer. The more anodic value seen for MWCNTs in comparison to MWCNTs-NH₂ is consistent with the greater catalytic activity of the former. On the basis of an analysis of reductive signals from both ensemble and single-entity data in the presence of oxygen, all results evidenced that the addition of N contents to carbon nanotubes played only a little role in improving the ORR activity, which mainly reflected the oxygen functionalities.

The electrocatalysis of the ORR by MWCNTs or MWCNTs-NH₂ has been compared using single-entity and ensemble electrochemistry, showing the role of surface oxygen functionalities to facilitate peroxide formation from oxygen in alkaline media. The functionalization with amino groups on the surface of CNTs does not cause a higher ORR activity. However, we note that these conclusions are specific to carbon nanotubes and the extension to the role of N doping in other nanomaterials³⁴ will require separate investigations with respect to both the materials and the source of the N used in the modification procedure.³⁵ In this quest, we believe that the combination of single-entity measurements with well-established voltammetric procedures will be extremely helpful and will be of generic value. We note that it is important to recognize that the value of rotating disk and rotating ring-disk electrodes in which the disk is modified by a porous layer has been questioned, as summarized by Sokolov et al.³⁶ and references therein. Although the rotation of the disk defines the transport to the exterior of the porous surface, the transport *within* a randomly distributed layer of particles of CNTs or other nanomaterials remains challenging to model in any general way. Sokolov et al.³⁶ and Kätelhön et al.³⁷ highlighted the views of Qiao et al.³⁸ in the context of the ORR, who noted the problems with rotating electrodes and porous layers and

asserted that “future studies are extremely desirable to develop a correct and accurate method...”. We suggest that the combination of single-entity electrochemistry with conventional voltammetry as reported in this paper meets this challenge.

■ ASSOCIATED CONTENT

SI Supporting Information

The Supporting Information is available free of charge at <https://pubs.acs.org/doi/10.1021/acscatal.2c02465>.

Experimental section, estimation of minimum number of layers of MWCNTs or MWCNTs-NH₂ drop-casted on GC electrodes, CVs of MWCNTs- or MWCNTs-NH₂-modified GCEs under degassed conditions, estimation of the number of quinones at a single CNT, CVs of MWCNTs- or MWCNTs-NH₂-modified GCEs in the presence of oxygen, chronoamperogram of a carbon-microwire electrode in the absence of CNTs, and calculation of the transport-limited current for single carbon nanotubes (PDF)

■ AUTHOR INFORMATION

Corresponding Author

Richard G. Compton – Department of Chemistry, Physical and Theoretical Chemistry Laboratory, Oxford University, Oxford OX1 3QZ, Great Britain; orcid.org/0000-0001-9841-5041; Email: richard.compton@chem.ox.ac.uk

Authors

Yuanyuan Lu – Department of Chemistry, Physical and Theoretical Chemistry Laboratory, Oxford University, Oxford OX1 3QZ, Great Britain; orcid.org/0000-0001-5869-9975

Xiuting Li – Institute for Advanced Study, Shenzhen University, Shenzhen, Guangdong 518060, People's Republic of China; orcid.org/0000-0003-0580-3112

Archana Kaliyaraj Selva Kumar – Department of Chemistry, Physical and Theoretical Chemistry Laboratory, Oxford University, Oxford OX1 3QZ, Great Britain

Complete contact information is available at: <https://pubs.acs.org/doi/10.1021/acscatal.2c02465>

Author Contributions

Y.L.: performed experiments, investigation, data analysis, and writing-original draft. X.L.: writing-review and editing. A.K.S.K.: writing-review and editing. R.G.C.: conceptualization, resources, supervision, and writing-review and editing.

Notes

The authors declare no competing financial interest.

■ REFERENCES

- (1) Steele, B. C. H.; Heinzel, A. Materials for fuel-cell technologies. *Nature* **2001**, 414 (6861), 345–352.
- (2) Chen, Z.; Yu, A.; Higgins, D.; Li, H.; Wang, H.; Chen, Z. Highly active and durable core-corona structured bifunctional catalyst for rechargeable metal-air battery application. *Nano Lett.* **2012**, 12 (4), 1946–1952.
- (3) Duan, J.; Chen, S.; Jaroniec, M.; Qiao, S. Z. Heteroatom-Doped Graphene-Based Materials for Energy-Relevant Electrocatalytic Processes. *ACS Catal.* **2015**, 5 (9), 5207–5234.
- (4) Zhang, J.; Sasaki, K.; Sutter, E.; Adzic, R. R. Stabilization of Platinum Oxygen-Reduction Electrocatalysts Using Gold Clusters. *Science* **2007**, 315 (5809), 220–222.
- (5) Greeley, J.; Stephens, I. E. L.; Bondarenko, A. S.; Johansson, T. P.; Hansen, H. A.; Jaramillo, T. F.; Rossmeisl, J.; Chorkendorff, I.; Nørskov, J. K. Alloys of platinum and early transition metals as oxygen reduction electrocatalysts. *Nat. Chem.* **2009**, 1 (7), 552–556.
- (6) Sasaki, K.; Shao, M.; Adzic, R. Dissolution and stabilization of platinum in oxygen cathodes. *Polymer electrolyte fuel cell durability* **2009**, 7–27.
- (7) Zheng, Y.; Jiao, Y.; Jaroniec, M.; Jin, Y.; Qiao, S. Z. Nanostructured metal-free electrochemical catalysts for highly efficient oxygen reduction. *Small* **2012**, 8 (23), 3550–3566.
- (8) Li, J. C.; Hou, P. X.; Liu, C. Heteroatom-doped carbon nanotube and graphene-based electrocatalysts for oxygen reduction reaction. *Small* **2017**, 13 (45), 1702002.
- (9) Dai, H. Carbon nanotubes: opportunities and challenges. *Surf. Sci.* **2002**, 500 (1), 218–241.
- (10) Dresselhaus, M. S.; Jorio, A.; Hofmann, M.; Dresselhaus, G.; Saito, R. Perspectives on carbon nanotubes and graphene Raman spectroscopy. *Nano Lett.* **2010**, 10 (3), 751–758.
- (11) Hu, C.; Dai, L. Carbon-based metal-free catalysts for electrocatalysis beyond the ORR. *Angew. Chem., Int. Ed.* **2016**, 55 (39), 11736–11758.
- (12) Pumera, M. The electrochemistry of carbon nanotubes: fundamentals and applications. *Chemistry* **2009**, 15 (20), 4970–4978.
- (13) Tammeveski, K.; Kontturi, K.; Nichols, R. J.; Potter, R. J.; Schiffrin, D. J. Surface redox catalysis for O₂ reduction on quinone-modified glassy carbon electrodes. *J. Electroanal. Chem.* **2001**, 515 (1), 101–112.
- (14) Yeager, E. Electrocatalysts for O₂ reduction. *Electrochim. Acta* **1984**, 29 (11), 1527–1537.
- (15) Gong, K.; Du, F.; Xia, Z.; Durstock, M.; Dai, L. Nitrogen-doped carbon nanotube arrays with high electrocatalytic activity for oxygen reduction. *Science* **2009**, 323 (5915), 760–764.
- (16) Kundu, S.; Nagaiah, T. C.; Xia, W.; Wang, Y.; Dommele, S. V.; Bitter, J. H.; Santa, M.; Grundmeier, G.; Bron, M.; Schuhmann, W.; et al. Electrocatalytic activity and stability of nitrogen-containing carbon nanotubes in the oxygen reduction reaction. *J. Phys. Chem. C* **2009**, 113 (32), 14302–14310.
- (17) Patil, I. M.; Reddy, V.; Lokanathan, M.; Kakade, B. Nitrogen and sulphur co-doped multiwalled carbon nanotubes as an efficient electrocatalyst for improved oxygen electroreduction. *Appl. Surf. Sci.* **2018**, 449, 697–704.
- (18) Chen, L.; Ren, J.; Yuan, Z. Insight into the Active Contribution of N-Coordinated Cobalt Phosphate Nanocrystals Coupled with Carbon Nanotubes for Oxygen Electrochemistry. *ACS Sustainable Chem. Eng.* **2021**, 9 (4), 1856–1866.
- (19) Zhao, H.; Sun, C.; Jin, Z.; Wang, D.; Yan, X.; Chen, Z.; Zhu, G.; Yao, X. Carbon for the oxygen reduction reaction: a defect mechanism. *Journal of Materials Chemistry A* **2015**, 3 (22), 11736–11739.
- (20) Maldonado, S.; Stevenson, K. J. Influence of Nitrogen Doping on Oxygen Reduction Electrocatalysis at Carbon Nanofiber Electrodes. *J. Phys. Chem. B* **2005**, 109 (10), 4707–4716.
- (21) Kätelhön, E.; Compton, R. G. Unscrambling illusionary catalysis in three-dimensional particle-modified electrodes: Reversible reactions at conducting particles. *Applied Materials Today* **2020**, 18, 100514.
- (22) Chen, L.; Kätelhön, E.; Compton, R. G. Particle-modified electrodes: General mass transport theory, experimental validation, and the role of electrostatics. *Applied Materials Today* **2020**, 18, 100480.
- (23) Li, X.; Batchelor-McAuley, C.; Whitby, S. A. I.; Tschulik, K.; Shao, L.; Compton, R. G. Single Nanoparticle Voltammetry: Contact Modulation of the Mediated Current. *Angew. Chem. Int. Edit* **2016**, 55 (13), 4296–4299.
- (24) Cheng, W.; Compton, R. G. Electrochemical detection of nanoparticles by ‘nano-impact’ methods. *TrAC Trends in Analytical Chemistry* **2014**, 58, 79–89.
- (25) Li, X.; Lin, C.; Batchelor-McAuley, C.; Laborda, E.; Shao, L.; Compton, R. G. New Insights into Fundamental Electron Transfer

from Single Nanoparticle Voltammetry. *J. Phys. Chem. Lett.* **2016**, *7* (8), 1554–1558.

(26) Lu, Y.; Li, X.; Compton, R. G. Oxygen Reduction Reaction at Single Entity Multiwalled Carbon Nanotubes. *J. Phys. Chem. Lett.* **2022**, *13*, 3748–3753.

(27) NanoLab Inc. Multiwall Carbon Nanotubes (Bamboo Structure) can be found at <https://www.nano-lab.com/bamboopowderd30l520.html/> (accessed 2022-06-21).

(28) XF NANO Advanced Materials Supplier Amino Modified Multiwall Carbon Nanotubes can be found at <https://en.xfnano.com/product/pro223.aspx/> (accessed 2022-06-21).

(29) Kaliyaraj Selva Kumar, A.; Zhang, Y.; Li, D.; Compton, R. G. A mini-review: How reliable is the drop casting technique? *Electrochem. Commun.* **2020**, *121*, 106867.

(30) Guin, P. S.; Das, S.; Mandal, P. C. Electrochemical Reduction of Quinones in Different Media: A Review. *International Journal of Electrochemistry* **2011**, *2011*, 1–22.

(31) Tammesveski, K.; Kontturi, K.; Nichols, R. J.; Potter, R. J.; Schiffrin, D. J. Surface redox catalysis for O₂ reduction on quinone-modified glassy carbon electrodes. *J. Electroanal. Chem.* **2001**, *515* (1–2), 101–112.

(32) Zhang, H.; Lin, C.; Sepunaru, L.; Batchelor-McAuley, C.; Compton, R. G. Oxygen reduction in alkaline solution at glassy carbon surfaces and the role of adsorbed intermediates. *J. Electroanal. Chem.* **2017**, *799*, 53–60.

(33) Lu, Y.; Li, X.; Compton, R. G. Oxygen Reduction Reaction at Single Entity Multiwalled Carbon Nanotubes. *J. Phys. Chem. Lett.* **2022**, *13*, 3748–3753.

(34) Pumera, M. Materials Electrochemists' Never-Ending Quest for Efficient Electrocatalysts: The Devil Is in the Impurities. *ACS Catal.* **2020**, *10* (13), 7087–7092.

(35) Wang, L.; Sofer, Z.; Pumera, M. Will Any Crap We Put into Graphene Increase Its Electrocatalytic Effect? *ACS Nano* **2020**, *14* (1), 21–25.

(36) Sokolov, S. V.; Sepunaru, L.; Compton, R. G. Taking cues from nature: Hemoglobin catalysed oxygen reduction. *Applied Materials Today* **2017**, *7*, 82–90.

(37) Kätelhön, E.; Chen, L.; Compton, R. G. Nanoparticle electrocatalysis: Unscrambling illusory inhibition and catalysis. *Applied Materials Today* **2019**, *15*, 139–144.

(38) Zhou, R.; Zheng, Y.; Jaroniec, M.; Qiao, S. Z. Determination of the Electron Transfer Number for the Oxygen Reduction Reaction: From Theory to Experiment. *ACS Catal.* **2016**, *6* (7), 4720–4728.

Recommended by ACS

Insights into the pH-dependent Behavior of N-Doped Carbons for the Oxygen Reduction Reaction by First-Principles Calculations

Mingpeng Chen, Tao Cheng, *et al.*

NOVEMBER 29, 2021
THE JOURNAL OF PHYSICAL CHEMISTRY C

READ 

Identification of Efficient Active Sites in Nitrogen-Doped Carbon Nanotubes for Oxygen Reduction Reaction

Zhengyu Xu, Paul W. Leu, *et al.*

FEBRUARY 26, 2020
THE JOURNAL OF PHYSICAL CHEMISTRY C

READ 

Intrinsic Catalytic Activity of Carbon Nanotubes for Electrochemical Nitrate Reduction

Nia J. Harmon, Hailiang Wang, *et al.*

JULY 14, 2022
ACS CATALYSIS

READ 

Mechanisms of Two-Electron and Four-Electron Electrochemical Oxygen Reduction Reactions at Nitrogen-Doped Reduced Graphene Oxide

Hyo Won Kim, Bryan D. McCloskey, *et al.*

DECEMBER 23, 2019
ACS CATALYSIS

READ 

Get More Suggestions >